A Stable, Magnetic, and Metallic Li 3 O 4 Compound as a Discharge Product in a Li–Air Battery

ARTICLE *in* JOURNAL OF PHYSICAL CHEMISTRY LETTERS · AUGUST 2014

Impact Factor: 7.46 · DOI: 10.1021/jz501160z

3 AUTHORS, INCLUDING:

Guo-Chun Yang
Northeast Normal University
105 PUBLICATIONS **1,144** CITATIONS
SEE PROFILE

Yanchao Wang
Jilin University
53 PUBLICATIONS **1,402** CITATIONS
SEE PROFILE

THE JOURNAL OF PHYSICAL CHEMISTRY Letters

Letter

pubs.acs.org/JPCL

A Stable, Magnetic, and Metallic Li_3O_4 Compound as a Discharge Product in a Li–Air Battery

Guochun Yang,[†,‡] Yanchao Wang,*[,†] and Yanming Ma*[,†]

[†]State Key Laboratory of Superhard Materials, Jilin University, Changchun 130012, China

[‡]Faculty of Chemistry, Northeast Normal University, Changchun 130024, China

Supporting Information

ABSTRACT: The Li–air battery with the specific energy exceeding that of a Li ion battery has been aimed as the next-generation battery. The improvement of the performance of the Li–air battery needs a full resolution of the actual discharge products. Li_2O_2 has been long recognized as the main discharge product, with which, however, there are obvious failures on the understanding of various experimental observations (e.g., magnetism, oxygen K-edge spectrum, etc.) on discharge products. There is a possibility of the existence of other Li–O compounds unknown thus far. Here, a hitherto unknown Li_3O_4 compound as a discharge product of the Li–air battery was predicted through first-principles swarm structure searching calculations. The new compound has a unique structure featuring the mixture of superoxide O_2^- and peroxide O_2^{2-}, the first such example in the Li–O system. The existence of superoxide O_2^- creates magnetism and hole-doped metallicity. Findings of Li_3O_4 gave rise to direct explanations of the unresolved experimental magnetism, triple peaks of oxygen K-edge spectra, and the Raman peak at 1125 cm^{-1} of the discharge products. Our work enables an opportunity for the performance of capacity, charge overpotential, and round-trip efficiency of the Li–air battery.

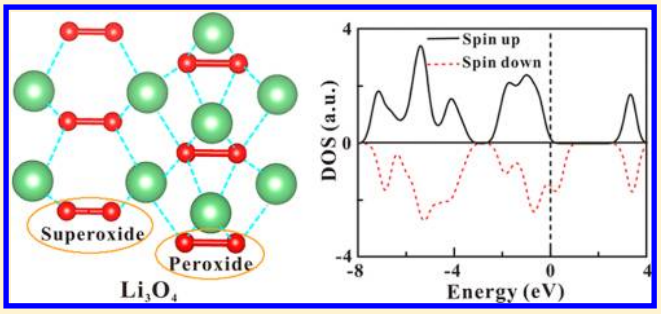

SECTION: Molecular Structure, Quantum Chemistry, and General Theory

As a primary energy resource, oil in total amount is rather limited, and the ever-increasing energy demand will not be satisfied in the long run. It is more problematic that oil consumption generates CO_2 and other pollutants. Clean and sustainable energy resources need to be developed in an effort to decrease our dependency on oil.[1,2] The rechargeable nonaqueous Li–air battery has received a great deal of interest in the past few years due to its extremely high specific energy, and it therefore has become one of the most promising candidates as an alternative energy resource for future electric vehicles.[3−9] However, the technology of nonaqueous Li–air batteries is still in its infancy, and key technical and scientific challenges remain to be overcome.[10−13]

The performance of the nonaqueous Li–air battery correlates closely with the structure, composition, and physical proprieties of the actual discharge products,[14−17] which are far from being well established.[18] Previous studies suggested commonly that Li_2O_2 is one of the discharge products.[14,19−21] However, X-ray diffraction (XRD) patterns of the discharge products are considerably broadened compared to that of standard Li_2O_2,[21−23] which may be attributed to poor crystallinity, structural defects, and/or composition non-stoichiometry of Li_2O_2.[22,23] Moreover, oxygen (O) or Li K-edge spectra showed that local environments of O and Li in the discharged electrodes are different from those of Li_2O_2. For example, there is a strong peak that appeared at 535 eV in the O K-edge spectra that is not observable in standard Li_2O_2. The origin of this strong peak remains unknown although it was postulated to arise from structural defects and/or the nonstoichiometry composition ($Li_{2-x}O_2$) of Li_2O_2.[22] More recently, an experimental study showed that the discharge products exhibit magnetism and a characteristic Raman peak at 1125 cm^{-1}, both of which were not shown in the standard Li_2O_2 sample. Subsequently, it was proposed that the magnetism and the unexplained Raman peak might be ascribed to the superoxide-like surface structure or nanocrystallization of Li_2O_2.[24] Another study even found that the discharge products contain two components, an oxygen-rich component with superoxide-like character and a Li_2O_2 component. The oxygen-rich superoxide-like component has a much smaller charge potential than the Li_2O_2 component. However, the actual structure and nature of the superoxide-like component are unknown.[23]

By all appearance, there is a necessity to re-examine the phase diagram of Li–O systems in an effort to explore other possible Li–O compounds, which are potential discharge products. In fact, Li_2O and LiO_2 have previously been proposed, but they were subsequently ruled out.[12,25] The

Received: June 8, 2014
Accepted: July 9, 2014

   dx.doi.org/10.1021/jz501160z | J. Phys. Chem. Lett. 2014, 5, 2516−2521

XRD pattern of Li_2O has a significant deviation from the experimental data of the discharge product.[26] LiO_2 is unstable at room temperature,[27] the operating temperature of a Li−air battery. Other stoichiometries in the Li−O system remain unknown thus far, but in view of the various puzzles related to the discharge product, they might be potentially important to the understanding of discharge products.

Here, we explore the entire phase diagram of the Li−O system by using the first-principles swarm-intelligence structural prediction calculations[28,29] unbiased by any prior known structures. A hitherto unknown Li_3O_4 compound was uncovered for the first time as a stable discharge product and found to exhibit intriguing half-metallic magnetism. The finding of Li_3O_4 enables the natural explanation of earlier unsolvable experimental observations. Our work represents a significant step forward toward the understanding of discharge products in a Li−air battery.

The phase stabilities of various Li_xO_y (x = 1−4, y = 1−4) compounds were investigated by calculating their formation energies at 0 K relative to the products of dissociation into constituent elements, as summarized in Figure 1. In general, a

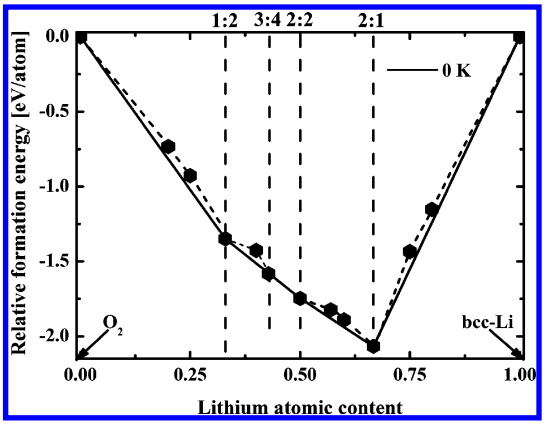

Figure 1. Relative formation energy with respect to solid Li and oxygen gas (O_2) for various Li−O stoichiometries at 0 K. The body-centered cubic (bcc) structure of elemental Li was used. Because Li has a light atomic mass, the zero-point energy was included in the formation energy calculations. The convex hulls are shown by solid lines. Dotted lines that directly connect data points are guides for the eyes.

structure whose formation energy lies on the convex hull (i.e., the phase stability line) is deemed stable with respect to decomposition into other Li−O compounds or elemental solids and thus can be experimentally synthesized.[30] As shown in Figure 1 at 0 K, the formation energy data of LiO_2, Li_3O_4, Li_2O_2, and Li_2O sit right on the convex hull, while that of Li_2O_3 is slightly above the convex hull. This indicates that under controllable experimental conditions, LiO_2, Li_3O_4, Li_2O_2, and Li_2O are synthesizable at low temperature. Note that the formation energy data were obtained by using the structures derived from our first-principles structure searching simulations, and they will be described in detail below. With the only input of chemical compositions in our CALYPSO structure searching calculations, the experimental antifluorite structure of Li_2O (space group $Fm3m$, four formula units per cell) and the hexagonal structure of Li_2O_2 (space group $P6_3/mmc$, two formula units per cell) were successfully reproduced, validating our structure searching methodology in application to the Li−O system.

The bulk crystalline structure of LiO_2 has not yet been fully resolved.[27] Most of the studies assumed the orthorhombic $Pnnm$ structure as obtained by replacing Na with Li for the known NaO_2 structure.[31−33] Our structure searching calculations unbiased by any prior known structure confirmed that the $Pnnm$ structure is indeed the most stable structure. The lattice parameters of the $Pnnm$ structure are summarized (Table S2, Supporting Information).

Our structure searching calculations identified a new stable Li_3O_4 compound with a hexagonal structure (space group $P\bar{6}m2$, one formula unit per cell; see Figure 2b). The structure

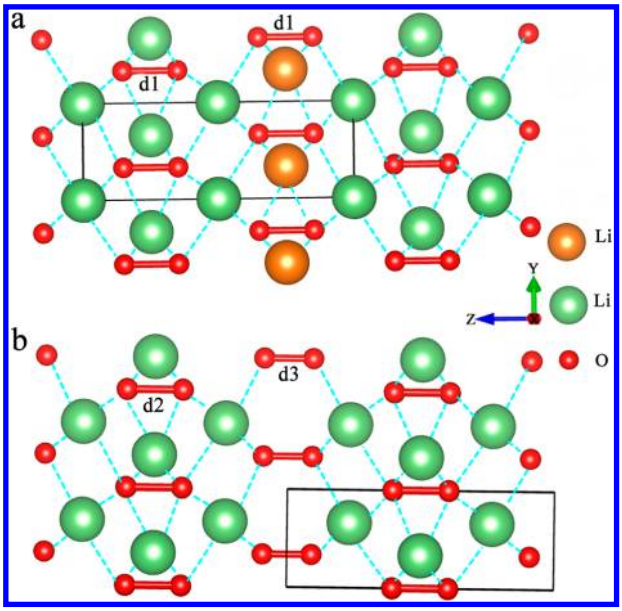

Figure 2. Crystal structures of Li_2O_2 (a) and Li_3O_4 (b). The solid rectangle represents one unit cell. The O−O distance ($d1$) in Li_2O_2 is 1.55 Å, while O−O distances ($d2$ and $d3$) in Li_3O_4 are 1.54 and 1.35 Å, respectively.

contains two inequivalent Li's occupying 2h (0.3333, 0.6667, 0.7671) and 1f (0.6667, 0.3333, 0.5000) positions and two inequivalent O's sitting at 2g (0.0000, 0.0000, 0.3956) and 2i (0.6667, 0.3333, 0.0914) sites. Each Li atom forms a six-fold coordination with O atoms, having three different Li−O distances of 1.97, 2.17, and 2.09 Å. All O atoms exist in quasi-molecular O_2 forms. There are two kinds of O_2 molecules with different intramolecular O−O bond lengths (1.35 and 1.54 Å), which are apparently longer than the bond length in gas-phase O_2 (1.21 Å).[34] These enlarged intramolecular bonds are easily understood because O_2 molecules in Li_3O_4 are negatively charged (Table S3, Supporting Information). The transferred charges from Li to O_2 occupy the anitbonding π^* orbitals of O_2 molecules to weaken and lengthen the intramolecular bond. Li_3O_4 is structurally very similar to Li_2O_2 (Figure 2a). The removal of brown Li atoms in Li_2O_2 leads to the formation of Li_3O_4 and thus shorter O−O bonds from $d1$ to $d3$. The shorter $d3$ bond length of 1.35 Å is within the length range (1.3−1.4 Å) of the superoxide O_2^-.[35] All of the intramolecular O−O bond lengths in Li_2O_2 are equal to 1.55 Å, a characteristic bond length for a peroxide O_2^{2-} seen also as the longer d2 bond in Li_3O_4. In this regard, the structure of Li_3O_4 can be well recognized as a mixture of superoxide O_2^- and peroxide O_2^{2-} groups. Note that our structural model of Li_3O_4 is

dx.doi.org/10.1021/jz501160z | J. Phys. Chem. Lett. 2014, 5, 2516−2521

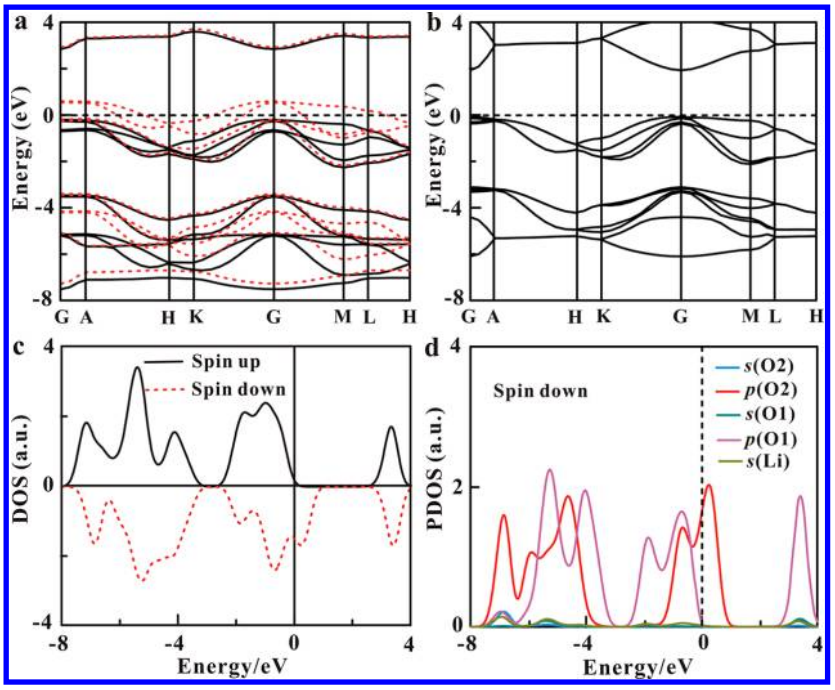

Figure 3. (a,b) Spin and electron band structures for Li_3O_4 and Li_2O_2, respectively. Spin-up and spin-down bands are shown in solid and dotted lines, respectively. (c) Spin DOS for Li_3O_4. (d) Projected spin-down DOS for Li_3O_4. O1 and O2 are within peroxide and superoxide groups, respectively. The dashed lines represent the Fermi levels.

fundamentally different from the earlier Li-vacancy or O-rich surface counterparts of Li_2O_2.[18,36−38]

To assess the phase stability of Li_3O_4 at room temperature, the quasi-harmonic model[39] was adopted to calculate the Gibbs free energy at 300 K through calculations of phonon spectra using the supercell method. The phonon results (Figure S1, Supporting Information) confirmed that the predicted Li_3O_4 structure is dynamically stable without showing any imaginary phonon modes. Because the considered temperature of 300 K is far below the melting temperatures (e.g., melting temperature at 1711 K for Li_2O),[40] the quasi-harmonic model should be rather valid. As a further test, the entropic curve of Li_2O was calculated to compare with the experimental data.[25] It is evident that theory matches nicely with experiment (Figure S2, Supporting Information). It is seen (Figure S3, Supporting Information) that Li_3O_4 is a thermodynamically stable phase at 300 K with respect to various dissociation routes into Li_2O_2 + O_2, Li_2O + O_2, and Li_2O_2 + LiO_2. From our calculations, Li_2O is the energetically most favorable stoichiometry, but it was seldom seen in the experiments on the discharge products.[12,25] This stemmed from the fact that the Li−air battery is working in O-rich conditions, where Li_3O_4 and Li_2O_2 are more stable with respect to Li_2O + O_2 (Figure S3, Supporting Information). Below, we focus on the discussion of the stable Li_3O_4 compound and its correlation with the discharge product.

The spin band structures for Li_3O_4 are depicted in Figure 3a. It can be clearly seen that Li_3O_4 exhibits a peculiar hole-doped metallic behavior. More intriguingly, a spin density of states (DOS) plot (Figure 3c) reveals novel half-metallic magnetism. The spin-up states are insulating, while the spin-down states are conducting. Analysis of the projected spin DOS suggested that the magnetism and conducting states arise from the superoxide O_2^- groups (Figure 3d). The same mechanism on the superoxide-induced magnetism and metallicity was also reported in the Li-vacancy or O-rich surfaces of Li_2O_2.[18,36] In an effort to better understand the hole-doped metallic behavior in Li_3O_4, the insulating band structures of Li_2O_2 are plotted in Figure 3b. Line shapes of Li_2O_2 resemble those of the spin-up energy band of Li_3O_4. Li acts as an electron donor, and the half depletion of Li out of Li_2O_2 leads to the substantial electron loss and thus lifts the spin-down states above the Fermi level. Magnetism and metallic holes are inevitably created. The appearance of magnetism in Li_3O_4 gives rise to the direct understanding of the experimental magnetism of the discharge product.[24]

The primitive unit cell of Li_3O_4 contains seven atoms. As a result, 18 optical phonon modes are expected at the zone center. Group theory analysis (Table S4, Supporting Information) showed that there are 10 Raman-active modes ($1E'' + 2E'' + 3A'_1 + 4E'$), 8 infrared-active modes ($4E' + 4A''_2$), and three silent modes ($3A''_1$). Of particular interest is the existence of a high-frequency Raman A'_1 vibration at 1101 cm^{-1}, which is not seen in standard Li_2O[41] and Li_2O_2[42] (Tables S5 and S6, Supporting Information). This high-frequency mode corresponds to the intramolecular O−O stretching vibration of the superoxide group (Figure S1, Supporting Information). It is interesting to find that the two Raman-active vibrations at 788 and 256 cm^{-1} of Li_2O_2 appeared also in Li_3O_4 (739 and 224 cm^{-1}). They are intimately related to the O−O vibrations of the peroxide group. The appearance of the characteristic Raman vibration at 1101 cm^{-1} in Li_3O_4 correlates nicely with the experimental Raman peak at 1125 cm^{-1} measured from the discharge product.[24]

The XRD spectra of various Li−O compounds (LiO_2, Li_2O, Li_3O_4, and Li_2O_2) were simulated (Figures 4a and S4, Supporting Information) to compare with the experimental data. Except for slight peak shifts, the major XRD features of Li_3O_4 are nearly identical to those of Li_2O_2, and fundamentally, they both can explain the experimental data. In contrast, LiO_2 and Li_2O have XRD patterns in substantial deviation with the

dx.doi.org/10.1021/jz501160z | J. Phys. Chem. Lett. 2014, 5, 2516−2521

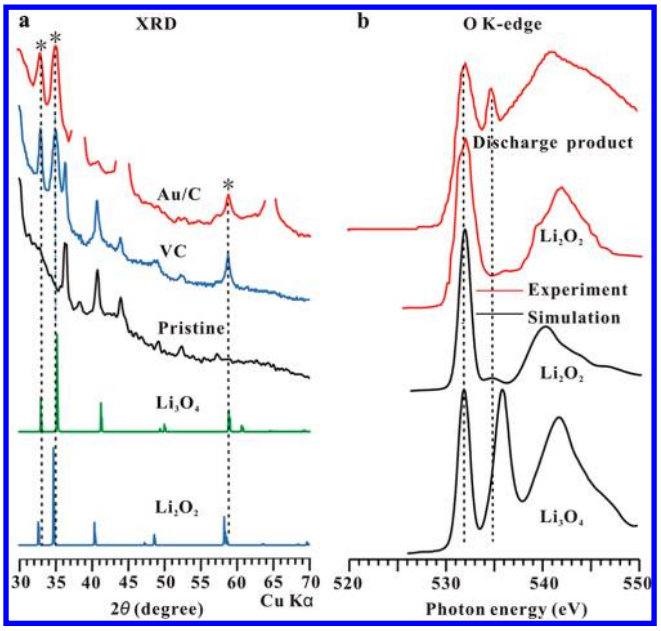

Figure 4. (a) The simulated XRD spectra of Li_2O_2 and Li_3O_4 to compare with the experimental data on discharge and pristine electrodes supported on a Celgard 480 separator (100 mA g_{carbon}^{-1}) for Vulcan carbon (VC) and Au-catalyzed Vulcan carbon (Au/C) (ref 22). The star symbols are indications of the characteristic peaks of the discharge products. (b) The simulated O K-edge spectra of Li_2O_2 and Li_3O_4 to compare with experimental data of discharged Au/C electrodes at 100 mA g_{carbon}^{-1} (ref 22).

experiments, and they thus should be ruled out as the discharge product. Further comparison (Figure S5, Supporting Information) was also made by using another experimental XRD measurement.[21]

The calculated O K-edge spectra for Li_2O_2 and Li_3O_4 together with the available experimental data[22] are shown in Figure 4b. The experimental spectrum of the pure Li_2O_2 sample was well reproduced by our calculations. The strong experimental peak at about 535 eV on the discharge product is apparently missing in the Li_2O_2 sample.[43,44] In contrast, Li_3O_4 accounts for this strong peak. Further analysis revealed that such a peak in Li_3O_4 originates from the intramolecular O−O bonding of the superoxide group (Figure S6, Supporting Information).

It is known that the decomposition of the electrolyte and the oxidation of the carbon matrix in the Li−air cell will form side products such as Li_2CO_3, HCO_2Li, and CH_3CO_2Li.[45,46] It is apparent that our finding of the Li_3O_4 compound is not the side products from the standpoint of IR, Raman, and XRD spectra (Figures S7 and S8, Supporting Information). Moreover, the Li_3O_4 compound with the half-metallic magnetism is greatly different from these side products, which are insulators.

By all above evidence, it is suggested that in addition to Li_2O_2, Li_3O_4 is deemed to exist as one of the discharge products. Unfortunately, we cannot determine the ratio between Li_2O_2 and Li_3O_4 based on our calculation, which needs further experimental confirmation. Moreover, our finding of Li_3O_4 is not against the fact that Li_2O_2 is the main discharge product because the coexistence of Li_2O_2 with Li_3O_4 does not contradict the experimental observation. A viable competition between Li_3O_4 and Li_2O_2 in the discharge product might be expected. First, energetically, Li_3O_4 and Li_2O_2 are competitive. The formation free energy of Li_3O_4 is −3.09 eV/Li, which is only slightly favorable over −3.01 eV/Li in Li_2O_2. Second, although both Li_2O_2 and Li_3O_4 can explain the experimental XRD data, the understanding of considerably broadened XRD spectra is still missing. If the contribution from both Li_2O_2 and Li_3O_4 is assumed, the broadened XRD feature is explainable (Figure S5, Supporting Information).[21]

Besides the thermodynamical stability of Li_3O_4, it is necessary to assess its electrochemical behavior because the electrochemical kinetics, that is, the overpotentials of formation, are also important to govern the actual formation of Li_3O_4 during the discharge process. We have explicitly calculated the electrochemical behavior of Li_3O_4 and Li_2O_2 through calculation of their reduction potentials (calculation details can be found in the Supporting Information). The obtained reduction potentials of Li_2O_2 (0.45 V) and Li_3O_4 (0.38 V) are rather similar. Therefore, the electrochemical behavior of Li_3O_4 has a great similarity to that of Li_2O_2. Because Li_2O_2 is reversible during the discharge and charge processes, we expect that Li_3O_4 might be also reversible.

It is known that the high resistance of Li_2O_2 limits greatly the rate capacity, results in high charge overpotential, and hampers the rechargeability of the Li−air battery.[14,47,48] Earlier studies suggested that electron transport can be enhanced by creation of Li-vacancy or O-rich surfaces of Li_2O_2.[18,36] However, the generation of a substantial amount of Li vacancies is unfavorable, and O-rich surfaces cannot offer a transportation path across the film.[49] The finding of metallic Li_3O_4 opens up the possibility for optimizing electron conduction to improve the performance of the Li−air battery. A proper control on the experimental condition to generate an optimal amount of Li_3O_4 in discharge products is greatly demanded.

In summary, the use of the advanced swarm structure searching technique allowed us to identify a hitherto unknown Li_3O_4 compound, which is energetically stable in O-rich conditions with respect to the dissociation into $Li_2O_2 + O_2$ and $Li_2O + O_2$. Li_3O_4 has a peculiar structural feature consisting of both superoxide O_2^- and peroxide O_2^{2-} groups, the only known mixed structure example so far in the Li−O system. The superoxide O_2^- groups induced the magnetism and the hole-doped metallicity of the system. The unresolved experimental observations on magnetism, the O K-edge spectrum, and the Raman peak at 1125 cm^{-1} were fundamentally understood. Our work represents a significant step forward toward the understanding of a Li−O phase diagram and possibly provides a pathway for optimizing the performance of the Li−air battery.

■ COMPUTATIONAL METHODS

Our structure searching simulations are performed through the CALYPSO structure prediction method[28,29] based on a particle swarm optimization algorithm via a global minimization of free-energy surfaces merging ab initio total energy calculations as implemented in the CALYPSO code,[28] which is unbiased by any prior known structural information. Our method has been benchmarked on various known systems, ranging from elements to binary and ternary compounds.[28,50−53] Detailed description of the method and predictions can be found in the Supporting Information.

Total energy calculations were performed in the framework of density functional theory within the generalized gradient approximation[54] as implemented in the VASP code.[55] The electron−ion interaction was described by means of a projector augmented wave with s^1p^0 and s^2p^4 electrons as valence for Li and O atoms, respectively. The cutoff energy of 700 eV and

dx.doi.org/10.1021/jz501160z | J. Phys. Chem. Lett. 2014, 5, 2516−2521

appropriate Monkhorst−Pack *k*-meshes were chosen to ensure that the total energy calculations were well converged to less than 1 meV/atom. The relative stability of different Li−O compounds at room temperature was calculated within a thermodynamic model[56] defined as $G(T) = G(T,N_{Li},N_O) - N_{Li}\mu_{Li}(T) - N_O\mu_O(T)$, where $G(T,N_{Li},N_O)$ are the Gibbs free energies of Li−O compounds and $\mu_{Li}(T)$ and $\mu_O(T)$ are the chemical potentials of Li and O atoms, respectively.

■ ASSOCIATED CONTENT

Supporting Information

The main structural parameters, the calculated Mulliken atomic charge, phonon entropy, phonon dispersion curve, vibrational frequency, simulated XRD, and O K-edge spectra. This material is available free of charge via the Internet at http://pubs.acs.org.

■ AUTHOR INFORMATION

Corresponding Authors

*E-mail: wyc@calypso.cn (Y.W.).
*E-mail: mym@jlu.edu.cn (Y.M.).

Notes

The authors declare no competing financial interest.

■ ACKNOWLEDGMENTS

This research was supported by the China 973 Program (2011CB808200), Natural Science Foundation of China under Nos. 11274136, 11104104, 11025418, and 91022029, the 2012 Changjiang Scholars Program of China, the Changjiang Scholar and Innovative Research Team in University (IRT1132), and the Postdoctoral Science Foundation of China under Grant 2013M541283.

■ REFERENCES

(1) Dresselhaus, M. S.; Thomas, I. L. Alternative Energy Technologies. *Nature* **2001**, *414*, 332−337.
(2) Garcia-Araez, N.; Novák, P. Critical Aspects in the Development of Lithium−Air Batteries. *J. Solid State Electrochem.* **2013**, *17*, 1793−1807.
(3) Oh, S. H.; Black, R.; Pomerantseva, E.; Lee, J.-H.; Nazar, L. F. Synthesis of a Metallic Mesoporous Pyrochlore as a Catalyst for Lithium−O_2 Batteries. *Nat. Chem.* **2012**, *4*, 1004−1010.
(4) Jung, H. G.; Hassoun, J.; Park, J. B.; Sun, Y. K.; Scrosati, B. An Improved High-Performance Lithium−Air Battery. *Nat. Chem.* **2012**, *4*, 579−585.
(5) Shui, J. L.; Okasinski, J. S.; Kenesei, P.; Dobbs, H. A.; Zhao, D.; Almer, J. D.; Liu, D. J. Reversibility of Anodic Lithium in Rechargeable Lithium−Oxygen Batteries. *Nat. Commun.* **2013**, *4*, No. 2255.
(6) Xu, J. J.; Wang, Z. L.; Xu, D.; Zhang, L. L.; Zhang, X. B. Tailoring Deposition and Morphology of Discharge Products towards High-Rate and Long-Life Lithium−Oxygen Batteries. *Nat. Commun.* **2013**, No. 2438.
(7) Chen, Y. H.; Freunberger, S. A.; Peng, Z. Q.; Fontaine, O.; Bruce, P. G. Charging a Li−O_2 Battery Using a Redox Mediator. *Nat. Chem.* **2013**, *5*, 489−494.
(8) Lu, Y. C.; Gasteiger, H. A.; Shao-Horn, Y. Catalytic Activity Trends of Oxygen Reduction Reaction for Nonaqueous Li−Air Batteries. *J. Am. Chem. Soc.* **2011**, *133*, 19048−19051.
(9) McCloskey, B. D.; Scheffler, R.; Speidel, A.; Bethune, D. S.; Shelby, R. M.; Luntz, A. C. On the Efficacy of Electrocatalysis in Nonaqueous Li−O_2 Batteries. *J. Am. Chem. Soc.* **2011**, *133*, 18038−18041.
(10) Choi, N.-S.; Chen, Z.; Freunberger, S. A.; Ji, X.; Sun, Y.; Amine, K. K.; Yushin, G.; Nazar, L. F.; Cho, J.; Bruce, P. G. Challenges Facing Lithium Batteries and Electrical Double-Layer Capacitors. *Angew. Chem., Int. Ed.* **2012**, *51*, 9994−10024.
(11) Christensen, J.; Albertus, P.; Sanchez-Carrera, R. S.; Lohmann, T.; Kozinsky, B.; Liedtke, R.; Ahmed, J.; Kojic, A. A Critical Review of Li/Air Batteries. *J. Electrochem. Soc.* **2012**, *159*, R1−R30.
(12) Lee, J. S.; Kim, S. T.; Cao, R.; Choi, N. S.; Liu, M.; Lee, K. T.; Cho, J. Metal−Air Batteries with High Energy Density: Li−Air versus Zn−Air. *Adv. Energy. Mater.* **2011**, *1*, 34−50.
(13) Bruce, P. G.; Freunberger, S. A.; Hardwick, L. J.; Tarascon, J. M. Li−O_2 and Li−S Batteries with High Energy Storage. *Nat. Mater.* **2012**, *11*, 19−29.
(14) Laoire, C. O.; Mukerjee, S.; Plichta, E. J.; Hendrickson, M. A.; Abraham, K. M. Rechargeable Lithium/TEGDME-LiPF_6/O_2 Battery. *J. Electrochem. Soc.* **2011**, *158*, A302−A308.
(15) Black, R.; Adams, B.; Nazar, L. F. Non-Aqueous and Hybrid Li−O_2 Batteries. *Adv. Energy Mater.* **2012**, *2*, 801−815.
(16) Cheng, F.; Chen, J. Metal−Air Batteries: From Oxygen Rduction Electrochemistry to Cathode Catalysts. *Chem. Soc. Rev.* **2012**, *41*, 2172−2192.
(17) Zhang, L. L.; Wang, Z. L.; Xu, D.; Zhang, X. B.; Wang, L. M. The Development and Challenges of Rechargeable Non-Aqueous Lithium−Air Batteries. *Int. Smart Nano Mater.* **2013**, *4*, 27−46.
(18) Radin, M. D.; Rodriguez, J. F.; Tian, F.; Siegel, D. J. Lithium Peroxide Surfaces Are Metallic, While Lithium Oxide Surfaces Are Not. *J. Am. Chem. Soc.* **2012**, *134*, 1093−1103.
(19) Abraham, K. M.; Jiang, Z. A Polymer Electrolyte-Based Rechargeable Lithium/Oxygen Battery. *J. Electrochem. Soc.* **1996**, *143*, 1−5.
(20) McCloskey, B. D.; Bethune, D. S.; Shelby, R. M.; Girishkumar, G.; Luntz, A. C. Solvents' Critical Role in Nonaqueous Lithium−Oxygen Battery Electrochemistry. *J. Phys. Chem. Lett.* **2011**, *2*, 1161−1166.
(21) Ogasawara, T.; Debart, A.; Holzapfel, M.; Novak, P.; Bruce, P. G. Rechargeable Li_2O_2 Electrode for Lithium Batteries. *J. Am. Chem. Soc.* **2006**, *128*, 1390−1393.
(22) Lu, Y. C.; Kwabi, D. G.; Yao, K. P. C.; Harding, J. R.; Zhou, J. G.; Zuin, L.; Shao-Horn, Y. The Discharge Rate Capability of Rechargeable Li−O_2 Batteries. *Energy. Environ. Sci.* **2011**, *4*, 2999−3007.
(23) Zhai, D. Y.; Wang, H. H.; Yang, J. B.; Lau, K. C.; Li, K. X.; Amine, K.; Curtis, L. A. Disproportionation in Li−O_2 Batteries Based on a Large Surface Area Carbon Cathode. *J. Am. Chem. Soc.* **2013**, *135*, 15364−15372.
(24) Yang, J.; Zhai, D.; Wang, H.; Lau, K. C.; Schlueter, J. A.; Du, P.; Myers, D. J.; Sun, Y. K.; Curtiss, L. A.; Amine, K. Evidence for Lithium Superoxide-Like Species in the Discharge Product of a Li−O_2 Battery. *Phys. Chem. Chem. Phys.* **2013**, *15*, 3764−3771.
(25) Shao, Y. Y.; Park, S.; Xiao, J.; Zhang, J. G.; Wang, Y.; Liu, J. Electrocatalysts for Nonaqueous Lithium−Air Batteries: Status, Challenges, and Perspective. *ACS Catal.* **2012**, *2*, 844−857.
(26) Lau, K. C.; Curtiss, L. A.; Greeley, J. Density Functional Investigation of the Thermodynamic Stability of Lithium Oxide Bulk Crystalline Structures as a Function of Oxygen Pressure. *J. Phys. Chem. C* **2011**, *115*, 23625−23633.
(27) Sangster, J.; Pelton, A. D. The Li−O (Lithium−Oxygen) System. *J. Phase Equilib.* **1992**, *13*, 296−299.
(28) Wang, Y.; Lv, J.; Zhu, L.; Ma, Y. Crystal Structure Prediction via Particle-Swarm Optimization. *Phys. Rev. B* **2010**, *82*, 094116.
(29) Wang, Y.; Lv, J.; Zhu, L.; Ma, Y. CALYPSO: A Method for Crystal Structure Prediction. *Comput. Phys. Commun.* **2012**, *183*, 2063−2070.
(30) Zhang, X.; Trimarchi, G.; Zunger, A. Possible Pitfalls in Theoretical Determination of Ground-State Crystal Structures: The Case of Platinum Nitride. *Phys. Rev. B* **2009**, *79*, 092102.
(31) Kang, S. Y.; Mo, Y. F.; Ong, S. P.; Ceder, G. A Facile Mechanism for Recharging Li_2O_2 in Li−O_2 Batteries. *Chem. Mater.* **2013**, *25*, 3328−3336.
(32) Seriani, N. Ab Initio Thermodynamics of Lithium Oxides: from Bulk Phases to Nanoparticles. *Nanotechnology* **2009**, *20*, 445703.

(33) Zhuravlev, Yu. N.; Obolonskaya, O. S. Structure, Mechanical Stability, and Chemical Bond in Alkali Metal Oxides. *J. Struct. Chem.* **2010**, *51*, 1005−1013.
(34) Haynes, W. M. *CRC Handbook of Chemistry and Physics*, 91st ed.; CRC Press (Taylor and Francis): Boca Raton, FL, 2011.
(35) Abrahams, S. C.; Kalnajs, J. The Crystal Structure of α-Potassium Superoxide. *Acta Crystallogr.* **1955**, *8*, 503−506.
(36) Hummelshoj, J. S.; Blomqvist, J.; Datta, S.; Vegge, T.; Rossmeisl, J.; Thygesen, K. S.; Luntz, A. C.; Jacobsen, K. W.; Norskov, J. K. Elementary Oxygen Electrode Reactions in the Aprotic Li−Air Battery. *J. Chem. Phys.* **2010**, *132*, 071101.
(37) Chen, J.; Hummelshoj, J. S.; Thygesen, K. S.; Myrdal, J. S. G.; Norkov, J. K.; Vegge, T. The Role of Transition Metal Interfaces on the Electronic Transport in Lithium−Air Batteries. *Catal. Today.* **2011**, *165*, 2−9.
(38) Hummelshøj, J. S.; Luntz, C.; Nørskov, J. K. Theoretical Evidence for Low Kinetic Overpotentials in Li−O_2 Electrochemistry. *J. Chem. Phys.* **2013**, *138*, 034703.
(39) Togo, A.; Oba, F.; Tanaka, I. First-Principles Calculations of the Ferroelastic Transition Between Rutile-Type and $CaCl_2$-Type SiO_2 at High Pressures. *Phys. Rev. B* **2008**, *78*, 134106.
(40) Greenwood, N. N.; Earnshaw, A. *Chemistry of the Elements*; Pergamon Press: Oxford, U.K., 1984; pp 97−99. ISBN: 0-08-022057-6.
(41) Lazicki, A.; Yoo, C.-S.; Evans, W. J.; Pickett, W. E. Pressure-Induced Antifluorite-to-Anticotunnite Phase Transition in Lithium Oxide. *Phys. Rev. B* **2006**, *73*, 184120.
(42) Débart, A.; Paterson, A. J.; Bao, J. L.; Bruce, P. G. α-MnO_2 Nanowires: A Catalyst for the O_2 Electrode in Rechargeable Lithium Batteries. *Angew. Chem., Int. Ed.* **2008**, *47*, 4521−4524.
(43) Karan, N. K.; Balasubramanian, B.; Fister, T. T.; Burrell, A. K.; Du, P. Bulk-Sensitive Characterization of the Discharged Products in Li−O_2 Batteries by Nonresonant Inelastic X-ray Scattering. *J. Phys. Chem. C* **2012**, *116*, 18132−18138.
(44) Chan, M. K. Y.; Shirley, E. L.; Karan, N. K.; Balasubramanian, M.; Ren, Y.; Greeley, J. P.; Fister, T. T. Structure of Lithium Peroxide. *J. Phys. Chem. Lett.* **2011**, *2*, 2483−2486.
(45) Freunberger, S. A.; Chen, Y.; Drewett, N. E.; Hardwick, L. J.; Bardé, F.; Bruce, P. G. The Lithium−Oxygen Battery with Ether-Based Electrolytes. *Angew. Chem., Int. Ed.* **2011**, *50*, 8609−8613.
(46) Freunberger, S. A.; Chen, Y.; Peng, Z. Q.; Griffin, J. M.; Hardwick, L. J.; Barde, F.; Novak, P.; Bruce, P. G. Reactions in the Rechargeable Lithium−O_2 Battery with Alkyl Carbonate Electrolytes. *J. Am. Chem. Soc.* **2011**, *133*, 8040−8047.
(47) Albertus, P.; Girishkumar, G.; McCloskey, B.; Sanchez-Carrera, R. S.; Kozinsky, B.; Christensen, J.; Luntz, A. C. Identifying Capacity Limitations in the Li/oxygen Battery Using Experiments and Modeling. *J. Electrochem. Soc.* **2011**, *158*, A343−A351.
(48) Viswanathan, V.; Thygesen, K. S.; Hummelshøj, J. S.; Nørskov, J. K.; Girishkumar, G.; McCloskey, B. D.; Luntz, A. C. Electrical Conductivity in Li_2O_2 and its Role in Determining Capacity Limitations in Non-Aqueous Li−O_2 Batteries. *J. Chem. Phys.* **2011**, *135*, 214704.
(49) Geng, W. T.; He, B. L.; Ohno, T. Grain Boundary Induced Conductivity in Li_2O_2. *J. Phys. Chem. C* **2013**, *117*, 25222−25228.
(50) Lv, J.; Wang, Y. C.; Zhu, L.; Ma, Y. M. Predicted Novel High-Pressure Phases of Lithium. *Phys. Rev. Lett.* **2011**, *106*, 015503.
(51) Zhu, L.; Wang, Z. M.; Wang, Y. C.; Zou, G. T.; Mao, H. K.; Ma, Y. M. Spiral Chain O_4 form of Dense Oxygen. *Proc. Natl. Acad. Sci. U.S.A.* **2012**, *109*, 751−753.
(52) Wang, H.; Tse, J.; Tanaka, K.; Iitaka, T.; Ma, Y. M. Superconductive Sodalite-Like Clathrate Calcium Hydride at High Pressures. *Proc. Natl. Acad. Sci. U.S.A.* **2012**, *109*, 6463−6466.
(53) Wang, Y. C.; Liu, H. Y.; Lv, J.; Zhu, L.; Wang, H.; Ma, Y. M. High Pressure Partially Ionic Phase of Water Ice. *Nat. Commun.* **2011**, *2*, 563−567.
(54) Perdew, J. P.; Chevary, J. A.; Vosko, S. H.; Jackson, K. A.; Pederson, M. R.; Singh, D. J.; Fiolhais, C. Atoms, Molecules, Solids, and Surfaces: Applications of the Generalized Gradient Gpproximation for Exchange and Correlation. *Phys. Rev. B* **1992**, *46*, 6671−6687.
(55) Kresse, G.; Furthmuller, J. Efficient Iterative Schemes For Ab Initio Total-Energy Calculations Using a Plane-Wave Basis Set. *Phys. Rev. B* **1996**, *54*, 11169−11186.
(56) Bollinger, M. V.; Jacobsen, K. W.; Nørskov, J. K. Atomic and Electronic Structure of MoS_2 Nanoparticles. *Phys. Rev. B* **2003**, *67*, 085410.